JACS
JOURNAL OF THE AMERICAN CHEMICAL SOCIETY
Article
pubs.acs.org/JACS

An Electrochemically Switched Smart Surface for Peptide Immobilization and Conformation Control

Jun Li,[†] Chun-Lin Sun,[†] Rong Shen,[‡] Xiao-Yan Cao,[†] Bo Zhou,[†] De-Cheng Bai,[‡] and Hao-Li Zhang*[,†]

[†]State Key Laboratory of Applied Organic Chemistry (SKLAOC), College of Chemistry and Chemical Engineering, [‡]School of Basic Medical SciencesLanzhou University, 222 Tianshui South Road, Lanzhou, 730000 China

Supporting Information

ABSTRACT: We report an electrochemically switched smart surface for controlled peptide immobilization and conformation control. This dynamic surface is based on self-assembled monolayers (SAMs) containing surface-bound trimethoxybenzene moieties, which can undergo electrochemically modulated surface activation to be stepwisely converted to two catechol derivatives. This new smart surface can be used to realize stepwise immobilization of a peptide, and more importantly, to control peptide conformation on a surface. We demonstrate herein that with one electrochemical activation step, a linear peptide containing an RGD sequence can be attached onto the SAMs. With the subsequence activation step, the attached linear RGD peptide can be converted into cyclic conformation. The SAMs bounded with linear and cyclic RGD exhibit different adhesion behaviors to fibroblasts cells. The reaction procedure can be well-monitored by cyclic voltammetry (CV), electrochemical surface enhanced Raman microscopy (EC-SERS), and X-ray photoelectron spectroscopy (XPS). It is believed this robust smart surface can find wide applications in surface immobilization of bioactive moieties.

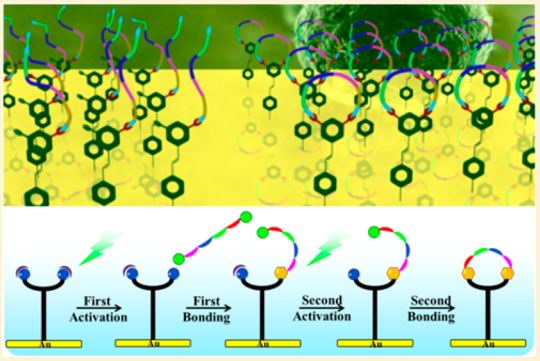

INTRODUCTION

Increasing efforts are being made to develop switchable surfaces with tunable surface functionality, which are also known as "smart surfaces".[1] Switchable surfaces that respond to external stimuli are important for a wide range of applications in fields such as molecular electronics, nanotechnology, and biodevices.[2] Many external factors including photon,[3] charge,[4] pH values,[5] temperature,[6] and chemical or electrochemical effects[7] have been used to initiate a variety of surface reactions.[2d,8]

Self-assembled monolayers (SAMs) on a metal surface provide convenient, flexible, and biocompatible system[9] and, therefore, have been applied to various biological applications, such as cell adhesion, arrays for biochips, and biosensors.[5b,8d,10] For most of these applications, the majority of SAMs-based biointerfaces offer only static surfaces with predetermined properties. Recent researches in the development of bioactive SAMs have tried to tackle the challenge of designing dynamic SAMs that could undergo on demand surface reactions under external stimuli.[3b,11] Such smart surfaces provide unique switchable monolayers whose surface activities can be turned on only when needed. These smart surfaces may enable new applications in fields like controlled ligand immobilization, cell adhesion, and biochemical sensors.[8c,9,12]

Smart surfaces that respond to electrochemical signals are particularly attractive from both fundamental and practical considerations, because electrochemistry technique can not only provide electrochemical stimuli for reaction control but also be used as a swift and sensitive analytical tool to monitor the surface reactions.[13] Electroactive SAMs on a gold surface have been extensively characterized and developed for a range of fundamental studies in biorelated applications.[2d,14] However, most of the reactive SAMs reported so far permit only one-step electrochemical modification. SAMs that enable multistep surface reactions under controlled conditions will significantly expand the applications of responsive surfaces.

Herein, a strategy for on demand electrochemically controlled multistep surface modification is described, which combines stepwisely electrochemical activations and surface heterocyclization reactions. This strategy utilizes SAMs containing trimethoxybenzene moieties that can be electrochemically converted twice into catechol-like moieties, and the generated catechol moieties can attach L-cysteine-containing peptides through a heterocyclization reaction. By using this strategy, we can easily realize immobilization of a peptide, and even control of peptide conformation on a surface.

EXPERIMENTAL SECTION

Materials. All the reagents and materials were purchased from commercial suppliers, and are of analytical grade. The electrodes for electrochemical experiments were purchased from Shanghai Chenhua Co., Ltd., China. All aqueous solutions were prepared with ultrapure water obtained with a Milli-Q System (Billerica, MA, U.S.A) with a resistivity of 18 MΩ·cm. Phosphate buffer solution (PBS) was prepared using K_2HPO_4 and KH_2PO_4, which was deaerated by purging

Received: May 14, 2014
Published: July 15, 2014

   dx.doi.org/10.1021/ja5048285 | J. Am. Chem. Soc. 2014, 136, 11050−11056

Scheme 1. Illustration of the Electrochemically Modulated Stepwise Modification on SAMs Surface[a]

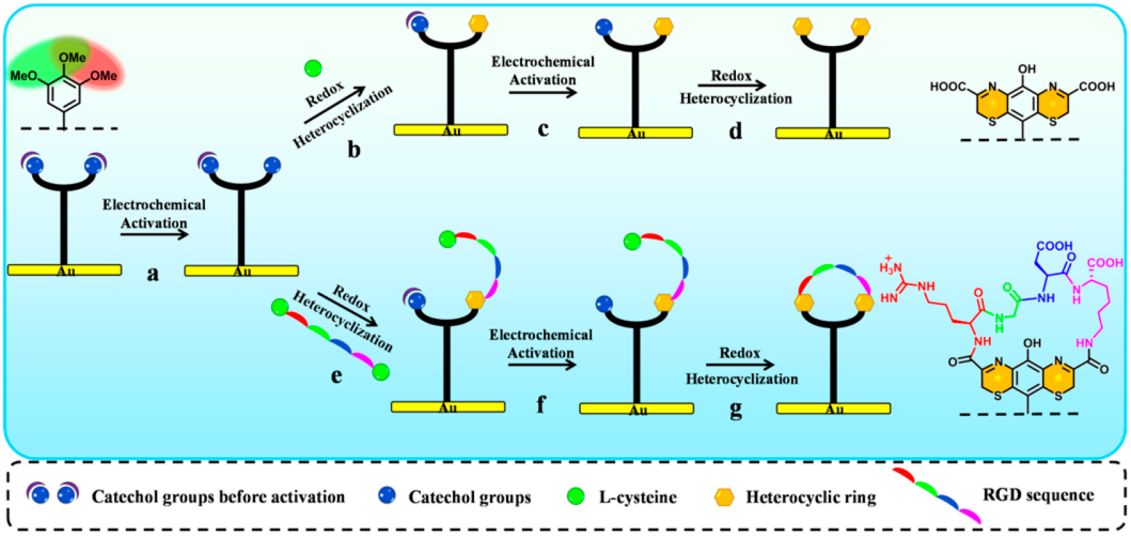

[a]In the trimethoxybenzene-terminated SAMs, every two adjacent methoxy groups can be regarded as a protected catechol linker. (a) The first electrochemical activation step; (b) attaching the first L-cysteine molecule; (c) the second electrochemical activation step; (d) attaching the second L-cysteine molecule; (e) attaching an L-cysteine-terminated linear RGD peptide; (f) the second electrochemical activation of the linear RGD peptide attached SAMs; (g) reaction with another terminal L-cysteine to give cyclic RGD peptide.

with nitrogen. The peptide acetyl-Cys-Arg-Gly-Asp-Lys-Cys (Ac-C-RGDK-C, which is abbreviated as RGD peptide) was obtained from Shanghai Biootech Bioscience and Technology Co., Ltd., China. All the experiments were carried out at room temperature, unless stated otherwise. The trimethoxybenzene terminated thiol, *trans*-3′,4′,5′-trimethoxy-4-mercaptostilbene, was synthesized following the procedure reported previously.[15]

Preparation of SAMs. The SAMs for electrochemical measurements were prepared on gold-coated glass chips (5 mm × 20 mm size), which were prepared by thermal evaporation of a 500 Å gold layer (99.99%) with a 50 Å chromium as the adhesion layer. Before being incubated in solutions of the thiols, the chips were carefully precleaned by repeated sonication in Millipore H_2O and ethanol for three times, respectively. The clean gold substrates were modified with SAMs by immersion in 10^{-4} M solutions of corresponding compounds in EtOH for 48 h at room temperature. The modified electrodes were further rinsed with ethanol to remove physically adsorbed molecules, and dried in nitrogen flow prior to further experiments.

Electrochemical Experiments. All electrochemical experiments were conducted with a computer-controlled CHI660 (CHI, U.S.A.) electrochemistry workstation. Working electrodes were gold-coated glass chips (5 mm × 20 mm size), used in conjunction with a Pt auxiliary electrode, and a saturated calomel electrode (SCE) reference electrode. The electrochemical surface enhanced Raman microscopy (EC-SERS) experiments were performed in an EC-SERS cell with three-electrode geometry, using a gold working electrode (2 mm diameter), a Pt counter electrode, and a silver wire as reference. Electrochemical activation of the initial SAMs was realized by scanning the potential between −0.1 and 0.9 V with a scan rate of 100 mV/s in 0.1 M H_2SO_4.

Preparation of SERS-Active Substrate. The gold disk electrode surface was first mechanically polished with alumina powders of 0.3 μm, 0.1 μm, and 0.05 μm, respectively, until a mirror-like surface was obtained. The electrode was rinsed and sonicated with ultrapure water to remove any adhering alumina. The gold electrode was cleaned for 10 min in piranha solution (H_2O_2 + H_2SO_4, 3:7 v/v; **caution**: highly erosive), followed by water rinsing, and then was electrochemically cleaned in 0.5 mol/L H_2SO_4 solution in the potential range of −0.2 and 1.5 V vs SCE. After rinsing with ultrapure water, the gold electrode was kept at −0.3 V in 0.1 mol/L KCl until the stabilization of the current. Then, the potential was scanned to 1.2 V at 1 V/s, set for 1.2 s for oxidation, then scanned back to −0.3 V at 0.5 V/s and set for 30 s for reduction. The cycle was repeated for 25 times, and the final potential should be −0.3 V to ensure a reduced state of the electrode. This roughening process results in an Au surface with a brown appearance.[16]

The electrochemical Surface Enhanced Raman Spectroscopy (EC-SERS). The EC-SERS experiment setup has been reported in our previous work.[17] SERS spectra were obtained using a confocal microscope Raman system (Renishaw in via Raman microscope) equipped with a Renishaw CCD camera. The microscope attachment is based on a Leica DM2500 M system with a 50× long-working-length objective, so that the objective will not be in contact with the electrolyte. A holographic notch filter was used to filter the exciting line, and two selective holographic gratings (1200 g/mm, 2400 g/mm) were employed, depending on the spectral resolution required. The exciting wavelength was 633 nm.

Cell Culture. Fibroblasts were cultured in Dulbecco's Modified Eagle Medium (Gibco) containing 10% calf bovine serum and 1% penicillin/streptomycin at 37 °C in a humidified atmosphere composed of 95% air and 5% CO_2. Cells were removed with a solution of 0.05% trypsin in 0.53 mmol/L EDTA, resuspended in serum-free medium (100,000 cells/mL) for cell seeding, and allowed 2 h to attach to the surface prior to the addition of serum-containing media. For passage, cells were resuspended in the same 10 mL of medium that they were growing in, and 3 mL was transferred to 7 mL of fresh medium in a new flask.

Cell Staining and Confocal Fluorescence Microscopy. Cells were cultured on gold-coated glass slides in a 12-well plate under normal culture conditions. After a 48 h incubation period, medium was removed. Then cells were fixed with 4% polyfluoroalkoxy (PFA) for 15 min and incubated with 0.01% acridine orange for 5 min, followed by two washes with PBS. The gold-coated glass slides were viewed by confocal fluorescence microscopy. Confocal fluorescence images were taken using a laser scanning confocal microscope LEICA TCS SP2.

RESULTS AND DISCUSSION

The stepwise surface modification strategy is illustrated in Scheme 1. The initial SAMs contain trimethoxybenzene terminal groups, which can be regarded as two protected 1,2-dihydroxybenzene (also known as catechol) groups, and are chemically inert. The trimethoxybenzene headgroup permits an electrochemical activation resulting in a catechol derivative

dx.doi.org/10.1021/ja5048285 | J. Am. Chem. Soc. 2014, 136, 11050−11056

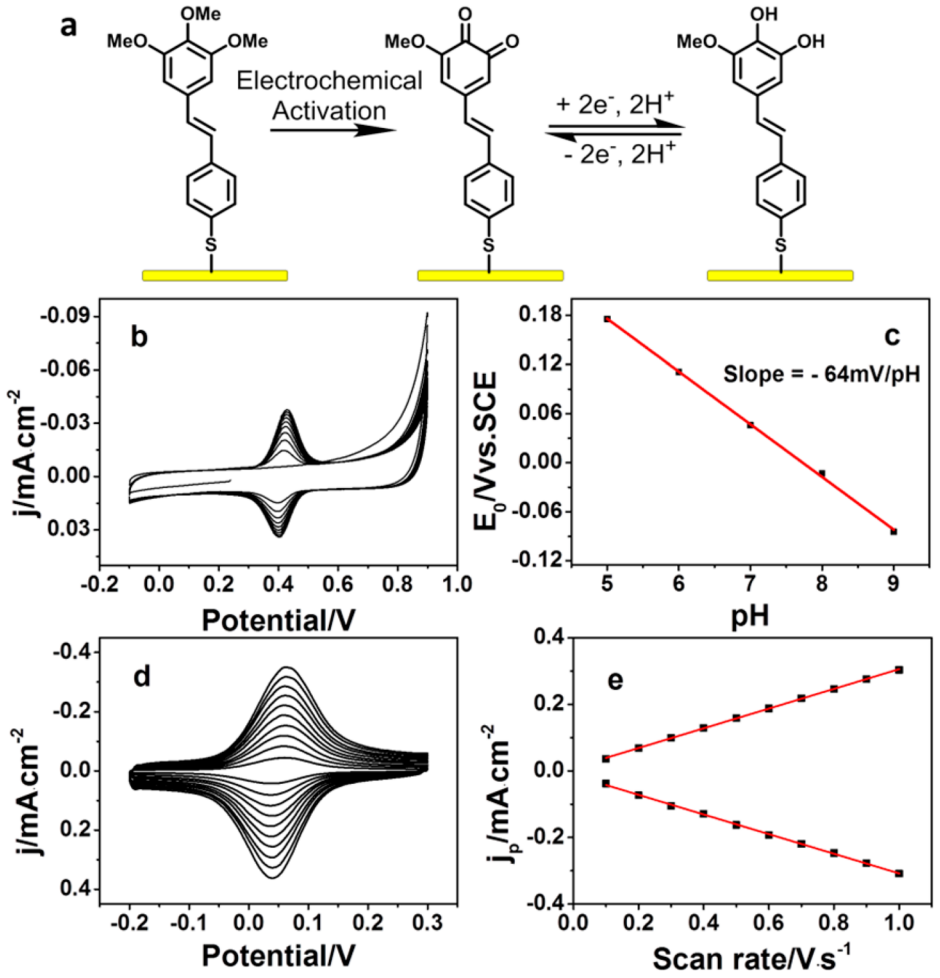

Figure 1. (a) Illustration of the process of the electrochemical activation reaction of the monolayer. (b) Sequence of cyclic voltammograms of the SAMs in 0.1 mol/L H_2SO_4. Scan number = 10. (c) Plots of E_0 vs pH. The E_0 was obtained from the midpoint of reduction and oxidation peak potentials from the cyclic voltammograms. (d) Voltammograms of the SAMs after electrochemical activation in PBS (pH: 7.4) for different scan rates (from 0.1 to 0.9 V/s). (e) The linear dependence of the peak current on the potential scan rate to highlight the presence of a surface-confined redox species.

(Scheme 1a). The catechol headgroup can then be electrochemically oxidized to 1,2-benzoquinone form, which could react with L-cysteine to form an electroinactive benzothiazine structure (Scheme 1b). This reaction is similar to the reaction between the surface-bound benzoquinone terminal group and L-cysteine reported before.[17] After the first surface heterocyclization reaction, a second electrochemical activation can be carried out, leading to the formation of a catechol derivative once again (Scheme 1c). After being oxidized to 1,2 benzoquinone, a second heterocyclization reaction takes place (Scheme 1d). It is noted that the L-cysteine for the second heterocyclization reaction can either come from solution or from the same peptide attached in the first step. In the latter case, the stepwise reaction leads to either linear or cyclic peptides immobilized onto the gold surface (Scheme 1e–g).

The proposed stepwise surface modification methodology has inherent advantages: first, the surface modifications are conducted under mild and biologically compatible conditions (pH: 7.4, 37 °C); second, every step can be readily monitored by electrochemical signal so that no other surface characterization technique is required; third, the surface modifications proceed under well-controlled conditions, which can be initiated and stopped at any step. Herein, we have used an RGD peptide with an L-cysteine subunit modified at both ends as an example, which can be regarded as a peptide containing two linkage units. We demonstrated that, by controlling the reaction to proceed in different steps, we can easily control the surface-bound RGD peptide to exist in linear or cyclic conformation.

The on-demand electrochemically controlled stepwise activation and the following heterocyclization reactions with L-cysteine have been monitored by cyclic voltammetry (CV) and EC-SERS. Figure 1a illustrates the activation process of the monolayer assembled on a gold electrode. Two adjacent methoxy groups of the trimethoxybenzene were first electrochemically activated to form a 1,2-benzoquinone-like structure, which can be reversibly reduced to a catechol-like structure by a $2e^- - 2H^+$ reaction.[18] Figure 1b shows the CVs recorded for the SAMs scanned at 100 mV/s between −0.1 and +0.9 V in 0.1 mol/L H_2SO_4. There was no obvious redox peak in the first scan segment, whereas an oxidation peak at E_{pa} = 0.439 V and a reduction peak at E_{pc} = 0.409 V were observed in the successive scans. A further increase in scan numbers led to a consecutive increase of peak currents but slight shifts of peak potentials. After 10 continuous scans, the redox peak current is stabilized with the anodic and the cathodic peaks being symmetric. The

dx.doi.org/10.1021/ja5048285 | J. Am. Chem. Soc. 2014, 136, 11050–11056

small separation between the oxidation and reduction peaks suggests that the electron-transfer kinetics between the catechol groups and the electrode is highly reversible, which can be attributed to the highly conjugated stilbene skeleton that permits fast electron transfer between the headgroup and the electrode.. The observed electrochemical response is consistent with previous work on conversion of 1,4-dimethoxybenzene into 1,4-benzoquinone moieties on the SAMs on a gold surface.[10c] It should be pointed out that other possible activation products, including 1,3-dihydroxybenzene (known as resorcinol) and trihydroxybenzene (known as pyrogallol), are known to exhibit only irreversible redox properties,[19] which is different from the CVs shown in Figure 1. This fact supports that the activation products of the trimethoxybenzene head groups in the SAMs are catechol derivatives.

To further confirm the activation product of the SAMs, we have conducted a series of control experiments (SI, Figure S1−5), in which the electrochemical properties of four molecules with the same stilbene skeleton were tested, including molecules that possess no $-OCH_3$ group (C1), one $-OCH_3$ group (C2), two $-OCH_3$ groups at the 1,3- (C3) and 1,2-position (C4), respectively (SI, Scheme S1). The CV curves from the SAMs of the control molecules C1, C2, and C3 give no appearance of any peak after 10 consecutive scans in 0.1 mol/L H_2SO_4 (SI, Figure S1−3), indicating that the arisen peaks of trimethoxybenzene-terminated SAMs can be assigned to neither the skeleton nor the resorcinol structure (the product after electrochemical activation of the $-OCH_3$ groups at the 1,3-position). The non-faradaic current in Figure S5 excludes the disturbance of bare gold electrode. However, with increased scans, the SAMs of C4 displayed slightly increased peak currents (SI, Figure S4), but the increasing rate is much slower than that of the trimethoxybenzene-terminated SAMs, suggesting that it is much more difficult to activate C4 compared to the trimethoxybenzene-terminated SAMs under the given conditions. This result demonstrates that the $-OCH_3$ group at the 3 position may accelerate the electrochemical activation process of the two $-OCH_3$ groups at the 1,2-positions. These control experiments lead to the conclusion that the electrochemical activation product of trimethoxybenzene-terminated SAMs is indeed the catechol derivative.

After electrochemical activation, CVs of the SAMs in PBS with different pH values and at different scan rates were recorded. Figure 1c presents the plots of E_0 (calculated by taking the average of the anodic and cathodic peak potentials) as a function of pH at the scan rate of 100 mV/s. From the plots, it can be inferred that an increase of pH value results in a decrease of E_0. The plot of E_0 as a function of pH value shows a slope equal to −64 mV/pH, very close to the theoretical value of −59 mV/pH for a $2e^{-1}-2H^+$ reaction.[20] CVs of the SAMs after electrochemical activation in PBS (pH: 7.4) as a function of scan rate are given in Figure 1d, which reveals that the current increases while the scan rate increases with no significant shift in peak position. Furthermore, as illustrated in Figure 1e, both the anodic and cathodic peak currents scale linearly with the scan rates, indicating that the redox behavior of the catechol headgroup is a surface-controlled reaction. The surface coverage (Γ, mol/cm^2) was calculated by integrating the area of the anodic or cathodic peak. The Γ for the trimethoxybenzene-terminated SAMs is calculated to be to 1.5×10^{-10} mol/cm^2, corresponding to a densely packed monolayer.

It is worth mentioning that it is not easy to synthesize and purify 1,2-benzoquinone derivatives containing thiol groups, because these two moieties may undergo Michael addition reaction,[21] whereas the compound *trans*-3′,4′,5′-trimethoxy-4-mercaptostilbene is easily synthesized and purified.[15] Therefore, our electrochemical approach for *in situ* generation of 1,2-benzoquinone-terminated SAMs has overcome the significant synthetic inconvenience for the thiol-teminated 1,2-benzoquinone derivative and avoids the possible side reaction between the thiol moieties and the headgroups. More importantly, this strategy can realize the stepwisely electrochemically modulated modification on the surface and facilely provides the desired electroactive SAMs for further study.

After electrochemical activation, the headgroups of the SAMs can present as either the catechol form under negative potentials, or the 1,2-benzoquinone form under positive potentials. To further verify this hypothesis, EC-SERS experiments were conducted to monitor the changes of the headgroups under different electrochemical conditions. Figure 2a presents the CV of the SAMs in PBS (pH: 7.4), in which the

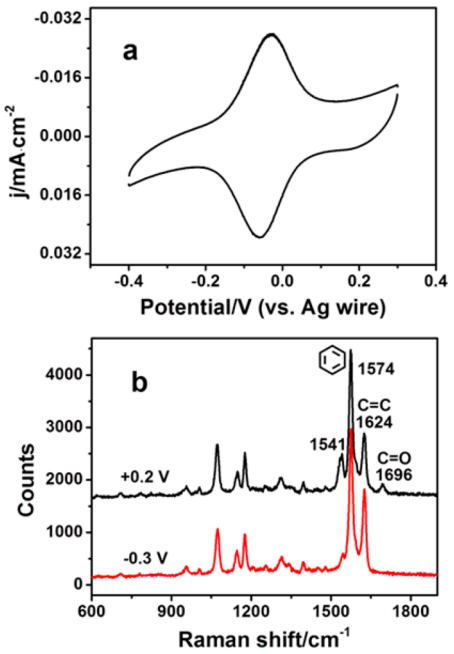

Figure 2. (a) Cyclic voltammograms of the SAMs in 0.2 mol/L PBS (pH: 7.4) after electrochemical activation. (b) EC-SERS spectra of the SAMs after electrochemical activation in PBS (pH: 7.4) under different potentials vs silver wire.

catechol groups undergo an oxidation process at −28 mV. The resulting 1,2-benzoquinone groups can be reduced at −58 mV, and the voltammetric response is reversible. Figure 2b shows the SERS spectra acquired under two different potentials in PBS (pH: 7.4) on a SERS-active gold electrode. The potential was scanned from −0.3 V to +0.2 V, such that the catechol evolves from its reduced state to the fully oxidized state (1,2-benzoquinone). The SERS bands change when the potential is changed to +0.2 V, which shows a clear peak due to the carbonyl group at the position of 1696 cm^{-1}, indicating that headgroups of the monolayer have transformed from catechol to 1,2-benzoquinone. After applying a reducing potential of −0.3 V, the SERS spectrum returns to that corresponding to catechol, indicating that electrochemically controlled trans-

dx.doi.org/10.1021/ja5048285 | J. Am. Chem. Soc. 2014, 136, 11050−11056

formation between catechol and 1,2-benzoquinone species is highly reversible. The Raman spectra of the trimethoxybenzene terminated thiol and its two states after the electrochemical activation were simulated using density functional theory (DFT) methods, as shown in Figure S7 in the SI. It can be seen that the simulated Raman spectra of these three molecules are well consistent with that acquired from the experiment. The EC-SERS spectra further affirm that the electrochemical activation product of the trimethoxybenzene-terminated SAMs is a catechol derivative.

The reactivity of the activated SAMs with L-cysteine has been studied by electrochemistry. As reported in the literature, 1,2-benzoquinone derivative can react with L-cysteine, resulting in a benzothiazine product, which does not process an electroactive center.[22] Therefore, the disappearance and reemergence of the redox center make it facile to monitor the whole process. As proposed above, after electrochemical activation, the headgroups of the SAMs are turned to the 1,2-benzoquinone derivative under positive potentials. The CVs of 1,2-benzoquinone-terminated SAMs in the solution containing 10^{-3} mol/L L-cysteine show that both the anodic and cathodic peaks decrease with consecutive scans (Figure 3a and SI, Figure S7), consistent with the production of an electroinactive 1,4-benzothiazine derivative (Figure 3b). Furthermore, consecutive CV scans of the SAMs with 1,4-benzothiazine headgroups at 100 mV/s between the potential of −0.1 and +0.9 V in 0.1 mol/L H_2SO_4 (SI, Figure S8) show an increasing peak current, indicating that the SAMs undergo electrochemical activation for the second time. The CV indicates that the activation generates new 1,2-benzoquinone derivatives as illustrated in Figure 3c,[23] which gives the distinct redox peaks. In contrast, in the control experiment, the SAMs composed of 1,2-dimethoxybenzene-terminated thiol (molecule C4, illustrated in Scheme S1 in the SI) can also be electrochemically activated in 0.1 mol/L H_2SO_4 (SI, Figure S4), and then react with L-cysteine (SI, Figure S10). However, the resulting SAMs cannot be electrochemically activated for the second time. As shown in Figure 3d, the reactivated SAMs can react with L-cysteine for the second time, resulting in another electroinactive structure. The second reaction process is accompanied by a decrease in the redox peak currents (SI, Figure S9). The resulting SAMs give no increasing redox peaks when tested in the electrochemical activation condition for the third time. It is noted that parts b and d of Figure 3 suggest that a small portion of the surface-bound catechol moieties did not react with L-cysteine under the electrochemical activation condition, which can be attributed to the spatial hindrance effect from the tightly packed monolayer structure. Based on the remaining redox peaks, there were 14.26% and 24.55% catechol-like species that did not react with L-cysteine in the first and second reactions, respectively. This result is consistent with the fact that the heterocyclic product of the second reaction is larger than that of the first reaction and, hence, induces more spatial hindrance in the monolayer.

The XPS spectra of the SAMs in different reaction steps are shown in Figure S11 in the SI. It can be seen that there is no N 1s peak in spectrum of the initial trimethoxybenzene SAMs. After electrochemical activation and reaction with L-cysteine for the first time, the N 1s peak arises, indicating the successful reaction with L-cysteine. After the second electrochemical activation step and subsequent reaction with L-cysteine, the SAMs spectrum shows a further increased N 1s signal, which is almost twice that after the first reaction. The XPS results again

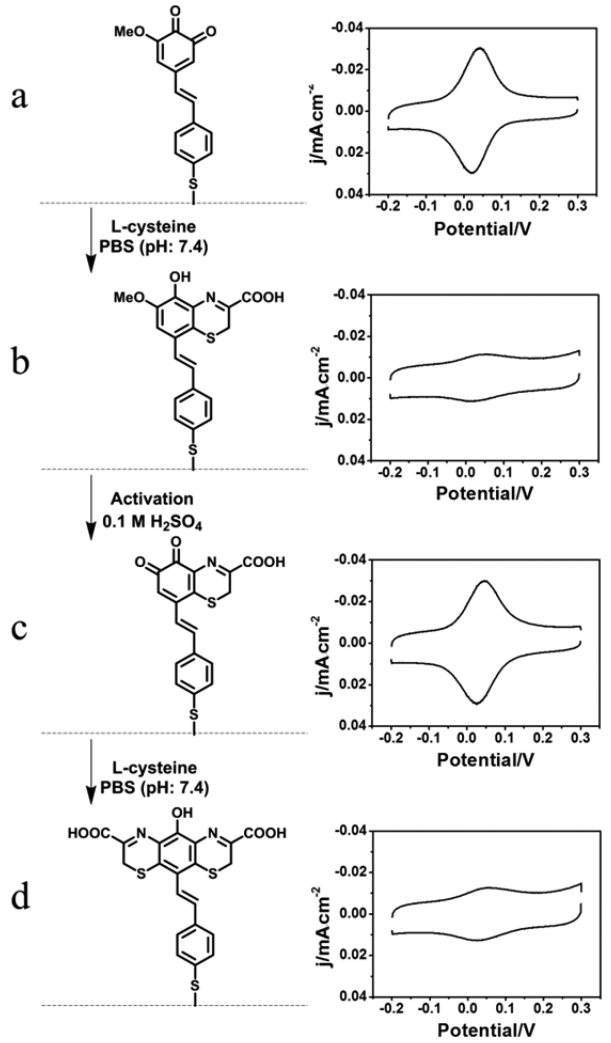

Figure 3. Electrochemical control and monitoring of the stepwise reactions in PBS (pH: 7.4) between L-cysteine and the monolayer. (a) The SAMs after the first electrochemical activation, in which the catechol to 1,2-benzoquinone interconversion can be monitored by the redox peaks at 65 mV and 92 mV. (b) Upon reaction with L-cysteine a 1,4-benzothiazine structure is formed, which is electroinactive. (c) The benzothiazine-containing structure can be electrochemically activated in 0.1 mol/L H_2SO_4 solution for the second time. The activation regenerates a new 1,2-benzoquinone derivative, which has distinct redox peaks. (d) The resulting SAMs can react with L-cysteine for the second time, ending in an electroinactive structure.

confirm that the trimethoxybenzene-terminated SAMs can be stepwisely activated and then react with L-cysteine.

Such stepwise surface reaction may have many applications, and one of them is to control the conformation of a peptide on a surface. To demonstrate this mechanism, we used the cell-adhesive RGD peptide as a dynamic ligand. It is well-known that affinity and specificity of RGD peptides for cell integrin receptors are strongly dependent on the conformation of the peptide backbone, and cyclic RGD peptides, in general, have a higher binding affinity (nM) than linear RGD peptides (μM).[24] We have used a linear RGD peptide containing L-cysteine units at both ends, in which one of the L-cysteine terminals is protected by an acetyl group. By controlling the electrochemical activation and heterocyclization steps for one or two times, the RGD sequence can be immobilized onto the SAMs with linear or cyclic conformations, respectively.

dx.doi.org/10.1021/ja5048285 | J. Am. Chem. Soc. 2014, 136, 11050−11056

The mixed SAMs composed of the trimethoxybenzene-terminated thiol and 2-(2-hydroxyethoxy)ethylethanethioate (DEG) (Figure 4a) were constructed by immersing freshly

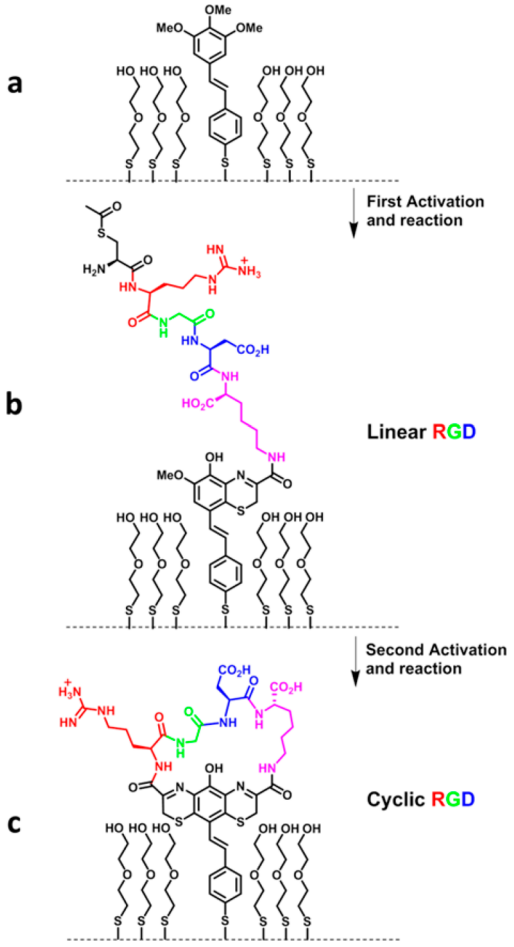

Figure 4. Electrochemically controlled attachment of linear and cyclic RGD peptide containing two terminal L-cysteine unites. (a) Structure of the mixed SAMs containing the trimethoxybenzene-terminated molecule and 2-(2-hydroxyethoxy)ethylethanethioate (DEG); (b) after electrochemical activation and reaction with the RGD peptide (Figure 4e), a linear RGD is attached onto the surface; (c) the linear RGD peptide can then be turned to be cyclic conformation after the second electrochemical activation and reaction.

evaporated gold surfaces in 10^{-4} mol/L total mixed thiol solution (1 mol % *trans*-3′,4′,5′-trimethoxy-4-mercaptostilbene and 99 mol % DEG), in slightly acidified ethanol, for 48 h at room temperature. The DEG is used to prevent nonspecific adsorption of protein.[25] The peak current after electrochemical activation of the mixed SAMs was much smaller than that of the single-component SAMs due to lower surface coverage of the trimethoxybenzene moieties (Figure S12a in the SI). The RGD peptide was installed via the first heterocyclization reaction to the surface in PBS (pH: 7.4) (Figure 4b). Because of the spatial hindrance of the peptide, the decrease of the peak current was slower than the reaction with L-cysteine (Figure S12b in the SI). The final CV of the SAMs after the reaction (Figure S12c in the SI in the SI) showed that there is scarcely any remaining catechol headgroups on the surface. Then the SAMs underwent electrochemical activation for the second time (Figure S12d in the SI). Afterward, the SAMs were immersed in a 0.5 mol/L H_2SO_4 solution for 2 h to remove the acetyl protection group from the RGD peptides. The surface was then placed in PBS (pH: 7.4) solution, and a set of consecutive CVs was conducted to promote the heterocyclization reaction for the second time. The decrease of the redox current became much slower than the first reaction step (Figure S12e in the SI), due to the much increased spatial hindrance effect for the cyclic RGD compared to the linear RGD and the low reaction probability. The final CV suggested that there is still a small amount of catechol headgroups remaining after the second reaction (Figure S12f in the SI). Compared with the SERS spectrum of initial mixed SAMs, the spectrum of SAMs after attaching with RGD peptide shows two more peaks, i.e. one peak at 1689 cm^{-1} due to the carbonyl group, and another peak at 1826 cm^{-1} that can be attributed to the carboxyl groups (Figure S13 in the SI). The XPS data also detect an obvious N 1s peak after the modification of RGD peptide, confirming the immobilization of RGD peptide.

To determine whether the on-surface peptide conformation changes would affect cell behavior, fibroblast cells were seeded on peptide surfaces presenting as linear or cyclic RGD. Cell behaviors were observed by using laser scanning confocal fluorescence microscopy. It is found that the average cell diameters are different on the SAMs with different RGD conformations. The cells spread more widely on SAMs containing cyclic RGD peptide than those containing linear RGD (Figure 5a,b). Figure 5c compares the average size of the

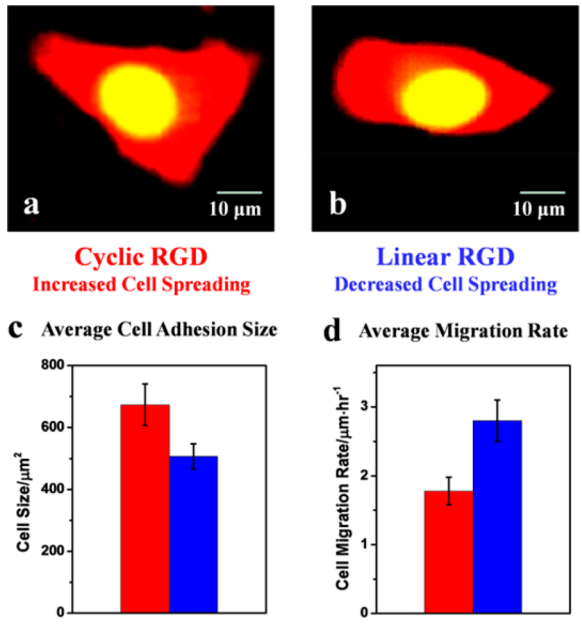

Figure 5. Representative confocal fluorescence images of stained fibroblast cells on the SAMs containing (a) cyclic RGD peptide (b) linear RGD peptide. (c) Cell spreading and (d) migration rates on SAMs containing cyclic and linear RDG peptide.

cells adhered on the two SAMs, which indicates that the cell sizes on the cyclic RGD surface are 33% larger than those of the cells on the linear RGD surface. In addition, cell migration measurement also indicates cells migrate more slowly on the more adhesive cyclic RGD surface, and the migration rate is 36% slower compared to that of cells on the linear RGD surface (Figure 5d). These observations are consistent with cell behavior observed on cyclic and linear RGD surfaces in previous work.[10d]

dx.doi.org/10.1021/ja5048285 | J. Am. Chem. Soc. 2014, 136, 11050−11056

CONCLUSION

We have developed a facile strategy to realize an on-demand stepwise modification on surfaces controlled by electrochemistry. The initial trimethoxybenzene-terminated SAMs on gold surface are electroinactive. After an electrochemical activation process, the SAMs generate a catechol-like redox center that can react with L-cysteine or L-cysteine-containing peptide. This reaction can be readily monitored by electrochemistry, EC-SERS, and XPS techniques. Then electrochemical activation and reaction with L-cysteine for the second time can be carried out to attach another L-cysteine-containing peptide. By using our stepwise electrochemical activation strategy, utilizing L-cysteine as a linkage, we have demonstrated a switchable surface that can be used to not only immobilize but also conduct conformation control of bioactive peptide. It is believed that this simple, efficient, and well-controlled smart surface may find applications in immobilizing and conformation control of peptide and protein on surfaces.

ASSOCIATED CONTENT

Supporting Information

Details of synthesis, XPS of the SAMs and other CVs. This material is available free of charge via the Internet at http://pubs.acs.org.

AUTHOR INFORMATION

Corresponding Author

haoli.zhang@lzu.edu.cn

Notes

The authors declare no competing financial interest.

ACKNOWLEDGMENTS

This work is supported by National Basic Research Program of China (973 Program) No. 2012CB933102, National Natural Science Foundation of China (NSFC 21233001, 21190034, 21172101), Specialized Research Fund for the Doctoral Program of Higher Education (SRFDP 20110211130001), the Fundamental Research Funds for the Central Universities and 111 Project.

REFERENCES

(1) Milner, S. T. *Science* **1991**, *251*, 905.

(2) (a) Zhu, M. Q.; Zhu, L.; Han, J. J.; Wu, W.; Hurst, J. K.; Li, A. D. *J. Am. Chem. Soc.* **2006**, *128*, 4303. (b) Rueckes, T.; Kim, K.; Joselevich, E.; Tseng, G. Y.; Cheung, C. L.; Lieber, C. M. *Science* **2000**, *289*, 94. (c) Pease, A. R.; Jeppesen, J. O.; Stoddart, J. F.; Luo, Y.; Collier, C. P.; Heath, J. R. *Acc. Chem. Res.* **2001**, *34*, 433. (d) Lamb, B. M.; Yousaf, M. N. *J. Am. Chem. Soc.* **2011**, *133*, 8870.

(3) (a) Abbott, S.; Ralston, J.; Reynolds, G.; Hayes, R. *Langmuir* **1999**, *15*, 8923. (b) Ichimura, K.; Oh, S.-K.; Nakagawa, M. *Science* **2000**, *288*, 1624.

(4) (a) Weissmüller, J.; Viswanath, R. N.; Kramer, D.; Zimmer, P.; Würschum, R.; Gleiter, H. *Science* **2003**, *300*, 312. (b) Luk, Y.-Y.; Abbott, N. L. *Science* **2003**, *301*, 623.

(5) (a) Matthews, J. R.; Tuncel, D.; Jacobs, R. M. J.; Bain, C. D.; Anderson, H. L. *J. Am. Chem. Soc.* **2003**, *125*, 6428. (b) Liu, D.; Bruckbauer, A.; Abell, C.; Balasubramanian, S.; Kang, D. J.; Klenerman, D.; Zhou, D. *J. Am. Chem. Soc.* **2006**, *128*, 2067.

(6) Arotçaréna, M.; Heise, B.; Ishaya, S.; Laschewsky, A. *J. Am. Chem. Soc.* **2002**, *124*, 3787.

(7) (a) Whitesides, G. M.; Grzybowski, B. *Science* **2002**, *295*, 2418. (b) Lahann, J.; Mitragotri, S.; Tran, T.-N.; Kaido, H.; Sundaram, J.; Choi, I. S.; Hoffer, S.; Somorjai, G. A.; Langer, R. *Science* **2003**, *299*, 371.

(8) (a) Liu, D.; Xie, Y.; Shao, H.; Jiang, X. *Angew. Chem., Int. Ed.* **2009**, *48*, 4406. (b) Minko, S.; Müller, M.; Motornov, M.; Nitschke, M.; Grundke, K.; Stamm, M. *J. Am. Chem. Soc.* **2003**, *125*, 3896. (c) Choi, I.; Kim, Y.-K.; Min, D.-H.; Lee, S.; Yeo, W.-S. *J. Am. Chem. Soc.* **2011**, *133*, 16718. (d) Seo, H.; Choi, I.; Lee, J.; Kim, S.; Kim, D. E.; Kim, S. K.; Yeo, W. S. *Chem.—Eur. J.* **2011**, *17*, 5804.

(9) Choi, I. S.; Chi, Y. S. *Angew. Chem., Int. Ed.* **2006**, *45*, 4894.

(10) (a) Yeo, W. S.; Yousaf, M. N.; Mrksich, M. *J. Am. Chem. Soc.* **2003**, *125*, 14994. (b) Yeo, W. S.; Min, D. H.; Hsieh, R. W.; Greene, G. L.; Mrksich, M. *Angew. Chem., Int. Ed.* **2005**, *44*, 5480. (c) He, X.-P.; Wang, X.-W.; Jin, X.-P.; Zhou, H.; Shi, X.-X.; Chen, G.-R.; Long, Y.-T. *J. Am. Chem. Soc.* **2011**, *133*, 3649. (d) Hoover, D. K.; Chan, E. W.; Yousaf, M. N. *J. Am. Chem. Soc.* **2008**, *130*, 3280. (e) Yeo, W. S.; Mrksich, M. *Langmuir* **2006**, *22*, 10816. (f) Ma, W.; Li, D.-W.; Sutherland, T. C.; Li, Y.; Long, Y.-T.; Chen, H.-Y. *J. Am. Chem. Soc.* **2011**, *133*, 12366.

(11) Kim, K.; Jeon, W. S.; Kang, J.-K.; Lee, J. W.; Jon, S. Y.; Kim, T.; Kim, K. *Angew. Chem., Int. Ed.* **2003**, *115*, 2395.

(12) Mendes, P. M. *Chem. Soc. Rev.* **2008**, *37*, 2512.

(13) (a) White, R. J.; Ervin, E. N.; Yang, T.; Chen, X.; Daniel, S.; Cremer, P. S.; White, H. S. *J. Am. Chem. Soc.* **2007**, *129*, 11766. (b) Erickson, D.; Liu, X.; Venditti, R.; Li, D.; Krull, U. J. *Anal. Chem.* **2005**, *77*, 4000. (c) Du, D.; Zou, Z.; Shin, Y.; Wang, J.; Wu, H.; Engelhard, M. H.; Liu, J.; Aksay, I. A.; Lin, Y. *Anal. Chem.* **2010**, *82*, 2989.

(14) (a) Saha, S.; Flood, A. H.; Stoddart, J. F.; Impellizzeri, S.; Silvi, S.; Venturi, M.; Credi, A. *J. Am. Chem. Soc.* **2007**, *129*, 12159. (b) Luo, W.; Westcott, N. P.; Pulsipher, A.; Yousaf, M. N. *Langmuir* **2008**, *24*, 13096. (c) Westcott, N. P.; Pulsipher, A.; Lamb, B. M.; Yousaf, M. N. *Langmuir* **2008**, *24*, 9237. (d) Love, J. C.; Estroff, L. A.; Kriebel, J. K.; Nuzzo, R. G.; Whitesides, G. M. *Chem. Rev.* **2005**, *105*, 1103. (e) Ulman, A. *Chem. Rev.* **1996**, *96*, 1533. (f) Ma, W.; Long, Y. T. *Chem. Soc. Rev.* **2013**, *43*, 30.

(15) Cao, X. Y.; Yang, J.; Dai, F.; Ding, D. J.; Kang, Y. F.; Wang, F.; Li, X. Z.; Liu, G. Y.; Yu, S. S.; Jin, X. L.; Zhou, B. *Chem.—Eur. J.* **2012**, *18*, 5898.

(16) Wu, D.-Y.; Li, J.-F.; Ren, B.; Tian, Z.-Q. *Chem. Soc. Rev.* **2008**, *37*, 1025.

(17) Li, J.; Sun, C. L.; Tan, L.; Xie, Y. L.; Zhang, H. L. *Langmuir* **2013**, *29*, 5199.

(18) Nguyen, N. H.; Esnault, C.; Gohier, F.; Bélanger, D.; Cougnon, C. *Langmuir* **2009**, *25*, 3504.

(19) (a) Nasr, B.; Abdellatif, G.; Cañizares, P.; Sáez, C.; Justo, L.; Rodrigo, M. A. *Environ. Sci. Technol.* **2005**, *39*, 7234. (b) Mu, S.; Chen, C. *J. Phys. Chem. C* **2012**, *116*, 3065.

(20) Petrangolini, P.; Alessandrini, A.; Berti, L.; Facci, P. *J. Am. Chem. Soc.* **2010**, *132*, 7445.

(21) Cao, K.; Stack, D. E.; Ramanathan, R.; Gross, M. L.; Rogan, E. G.; Cavalieri, E. L. *Chem. Res. Toxicol.* **1998**, *11*, 909.

(22) Napolitano, A.; Panzella, L.; Leone, L.; D'Ischia, M. *Acc. Chem. Res.* **2012**, *46*, 519.

(23) Trammell, S. A.; Moore, M.; Schull, T. L.; Lebedev, N. *J. Electroanal. Chem.* **2009**, *628*, 125.

(24) (a) Samanen, J.; Ali, F.; Romoff, T.; Calvo, R.; Sorenson, E.; Vasko, J.; Storer, B.; Berry, D.; Bennett, D. *J. Med. Chem.* **1991**, *34*, 3114. (b) Pfaff, M.; Tangemann, K.; Muller, B.; Gurrath, M.; Muller, G.; Kessler, H.; Timpl, R.; Engel, J. *J. Biol. Chem.* **1994**, *269*, 20233.

(25) Wang, R. L. C.; Kreuzer, H. J.; Grunze, M. *J. Phys. Chem. B* **1997**, *101*, 9767.